Electric-field-induced strain mechanisms in lead-free 94 % (Bi 1 / 2 Na 1 / 2) TiO 3 – 6 % BaTiO 3

Hugh Simons, John Daniels, Wook Jo, Robert Dittmer, Andrew Studer, Maxim Avdeev, Jürgen Rödel, and Mark Hoffman

Articles you may be interested in

Electric-field-induced strain mechanisms in lead-free 94%(Bi$_{1/2}$Na$_{1/2}$)TiO$_3$−6%BaTiO$_3$

Hugh Simons,[1,a)] John Daniels,[1] Wook Jo,[2] Robert Dittmer,[2] Andrew Studer,[3] Maxim Avdeev,[3] Jürgen Rödel,[2] and Mark Hoffman[1]

[1]*School of Materials Science and Engineering, The University of New South Wales, New South Wales 2052, Australia*
[2]*Institute of Materials Science, Technische Universität Darmstadt, Darmstadt 64287, Germany*
[3]*Bragg Institute, Australian Nuclear Science and Technology Organisation, Lucas Heights, New South Wales 2234, Australia*

High resolution neutron diffraction has been used to investigate the structural origin of the large electric-field-induced remanent strain in 94(Bi$_{1/2}$Na$_{1/2}$)TiO$_3$−6BaTiO$_3$ ceramics. The virgin material was found to be a mixture of near-cubic phases with slight tetragonal and rhombohedral distortions of $a^0a^0c^+$ and $a^-a^-a^-$ octahedral tilt type, respectively. Application of an electric field of 4.57 kV/mm transformed the sample to a predominantly rhombohedral $a^-a^-a^-$ modification with a significantly higher degree of structural distortion and a pronounced preferred orientation of the c-axis along the field direction. These electric field-induced structural effects contribute significantly to the macroscopic strain and polarization of this system. © *2011 American Institute of Physics.* [doi:10.1063/1.3557049]

Piezoelectric ceramics of the system $(1-x)$ $\times$(Bi$_{1/2}$Na$_{1/2}$)TiO$_3$−(x)BaTiO$_3$ (BNT-xBT) have drawn attention of late as lead-free alternatives to lead zirconate titanate (PZT).[1,2] The system contains a morphotropic phase boundary (MPB) between rhombohedral and tetragonal structures at 5–7 mol % BT,[3–5] where nearby compositions possess enhanced properties suitable for actuator and transducer applications (see Table I). Interestingly, these properties arise despite a pseudocubic structure at ambient conditions, suggesting an electric-field-induced phase transformation to a lower-symmetry structure.[5,7–15] Macroscopic strain measurements of 94BNT-6BT during the poling procedure show a remanent strain of approximately 0.34%. The investigation presented here is to identify the structural nature of this remanent strain.

Distortions of perovskite (ABO$_3$) structures such as BNT-BT involve tilting of the BO$_6$ octahedra and/or displacement of A- or B-site cations. These distortions are generally coupled, with one implying the other. Glazer notation[16] is used to describe octahedral tilting as a combination of rotations around the a, b, and c unit cell axes. Tilt components of unequal magnitude are assigned different letters, each followed by either +, −, or 0 to denote whether the rotation of adjacent octahedral layers is in-phase, antiphase, or absent, respectively. The $a^0a^0c^+$ and $a^-a^-a^-$ tilting systems reported for pure BNT and their associated unit-cell parameters are illustrated in Fig. 1, compared to the undistorted cubic form.

Pure BNT has a rhombohedral distortion and $a^-a^-a^-$ tilt system from 5–528 K,[17–19] though recent studies[13] have since suggested a monoclinic space group. A tetragonal $a^0a^0c^+$-tilted phase emerges at 528 K, creating a phase mixture until 673 K, above which the structure is a single phase of tetragonal $a^0a^0c^+$. The local structure of the mixed-phase region was originally assumed a coexistence

of tetragonal and rhombohedral nanodomains,[17,20,21] however, recent transmission electron microscopy (TEM) studies have proposed an intermediate, modulated orthorhombic phase from which the tetragonal phase nucleates.[18,19,22] At 773 K a cubic phase is first observed.[17,18,20] The cubic phase fraction increases until 813 K, where the structure becomes wholly cubic. These three phases differ only slightly in their unit cell parameters, making confident structural determination of small-grained polycrystalline samples challenging.

Synchrotron x-ray studies of BNT-7BT under applied electric fields revealed splitting of the (002)/(002) peaks and a tetragonal distortion nucleating from the pseudocubic structure which contributed to the macroscopic strain.[7,14] Similarly, various x-ray diffraction studies have revealed induced tetragonal distortions in Mn-doped BNT-5.6BT,[8] BNT-6BT,[11] and BNT-20BKT,[12] while Kling *et al.*[9] and Hinterstein *et al.*[10] used TEM and neutron diffraction to show a reversible electric-field-induced rhombohedral distortion in (Bi$_{1/2}$Na$_{1/2}$)TiO$_3$-6%BaTiO$_3$-3%(K$_{1/2}$Ni$_{1/2}$)NbO$_3$ (BNT-6BT-3KNN) and BNT-6BT-2KNN, respectively. Neutron

TABLE I. Electromechanical properties of 94BNT-6BT in comparison to commercially available PZT (PIC151). Note: comparing large-signal properties is difficult since 94BNT-6BT generates macroscopic strain via induced phase transformations as opposed to domain volume fraction changes in conventional piezoceramics.

	94BNT-6BT	PZT (PIC151)
ε_r	1726/881[a]	1667/2660[b]
d$_{33}$ (pC/N)	148	518
P$_{max}$ (μC/cm^2)	46	42
P$_{rem}$ (μC/cm^2)	39	36
S$_{max}$ (%)	0.5	0.52
S$_{rem}$ (%)	0.34	0.22
E$_c$ (kV/mm)	3.1	0.9

[a]All values measured at 50 mHz, poling completed at 6 kV/mm.
[b]Permittivity values refer to poled/unpoled.
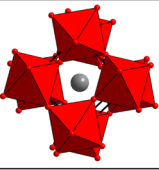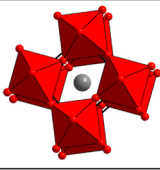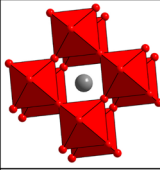
a)Electronic mail: h.simons@unsw.edu.au.

Space Group	Rhombohedral (R3c)	Tetragonal (P4bm)	Cubic (Pm$\bar{3}$m)
Structure			
Glazer System	$a^-a^-a^-$	$a^0a^0c^+$	$a^0a^0a^0$
a,c,α,β,γ	5.489,13.51,90,90,120	5.518,3.907,90,90,90	3.914,3.914,90,90,90

FIG. 1. (Color online) Structural properties of the rhombohedral, tetragonal, and cubic phases reported for pure BNT (see Ref. 4).

diffraction is more sensitive to light atom positions (i.e., oxygen) in the presence of heavy atoms than x-ray diffraction, and is therefore, more capable of detecting octahedral tilting. This technique was subsequently used to determine the effects of electrical poling on the structure of BNT-6BT. Our results show that electric-field-induced phase transformations occur via simultaneous lattice distortion and changes to the superlattice octahedral tilt system. By reducing structural symmetry and inducing a strong domain texture, this transformation generates significant macroscopic strain.

The scattering experiments used square-sectioned bars of composition 94BNT-6BT and dimensions $3.5 \times 3.5 \times 30$ mm^3 (± 0.05 mm tolerance). The initial powder was prepared via the conventional oxide/carbonate solid state processing route, using stoichiometric quantities of reagent-grade constituents (Alfa Aesar GmbH & Co KG, Karlsruhe, Germany) following the process detailed by Zhang *et al.*[15] After calcination at 900 °C, the reacted powder was ball-milled in ethanol, deagglomerated, and uniaxially pressed into $5 \times 5 \times 40$ mm^3 green bars. These were hydrostatically pressed to 300 MPa for 30 s and sintered at 1150 °C for 3 h. All external surfaces were ground and polished to a 3 μm finish. A 25 nm thick gold film was then sputtered onto two opposing 3.5×30 mm^2 surfaces.

The structure of the virgin material was determined via high-resolution neutron powder diffraction (HRPD) using the Echidna instrument (Bragg Institute, ANSTO)[23] with a wavelength of 1.622 Å. Data was collected over a period of 3 h. The major peaks in Fig. 2 describe a pseudocubic structure with a lattice parameter of 3.918 Å. (3/2 1/2 0) and (3/2 1/2 1/2) superlattice reflections indicate coexisting $a^0a^0c^+$ and $a^-a^-a^-$ tilt systems, although weak intensity suggests only minor deviation from cubic symmetry, supporting published structural data for similar materials.[8,9,24]

The sample was electrically poled at 25 °C by applying a dc voltage in 2 kV and 3 min increments to a maximum voltage of 16 kV (4.57 kV/mm). The voltage was then decremented to 0 kV in the same manner. After allowing the sample to relax for 1 h, the texture was measured on Echidna at a wavelength of 2.44 Å. The sample was rotated about the vertical axis (ω) over 180°, collecting patterns in 10° increments (see Fig. 3). After assuming structural symmetry about 180°, the data was corrected so that each pattern correlated with a particular angular difference, η, between the scattering and electric field vectors. Thus, structural change can be determined as a function of angle to electric field.

The poled sample was strongly textured (see Fig. 4), containing orientation-dependent changes to almost all peaks. Interestingly, the $a^0a^0c^+$ superlattice reflections seen
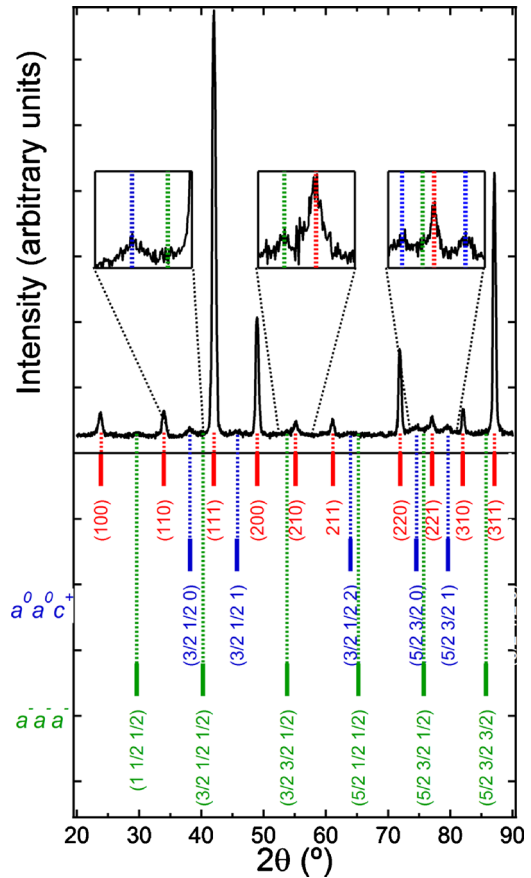
FIG. 2. (Color online) HRPD pattern collected at a wavelength of 1.622 Å. Peak indexing shows contributions from the $a^0a^0c^+$ and $a^-a^-a^-$ tilt-systems, respectively.

in the virgin sample were no longer present while the $a^-a^-a^-$ reflections were considerably stronger, confirming previously reported results,[9,10] where macroscopic domain formation was correlated with a field-induced transformation from *P4bm* to *R3c*. The (3/2 1/2 1/2) reflection was present across the entire range, though the maximum intensity was at 90° to the electric field. This indicates that the $a^-a^-a^-$ tilt system was induced in all grain orientations while the changing intensity suggests that the magnitude and/or the population of the distortion changes with respect to the grain angle to the electric field vector. Based on the rightwards shift in this peak, it also appears that the plane-spacing is reduced when oriented at 90° to the electric field. However, this is attributed to the coinciding lattice distortion.
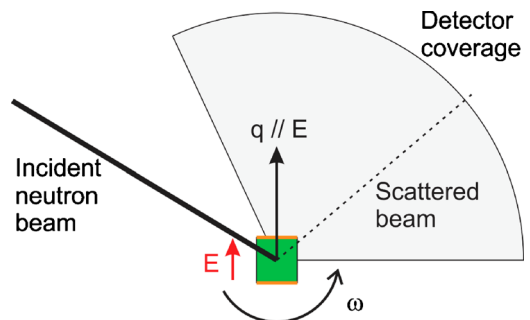
FIG. 3. (Color online) Schematic diagram of neutron diffraction setup. The vector *E* represents the poling direction. For a given scattered beam at a given rotation angle, ω, the scattering vector makes an angle to the poling direction.
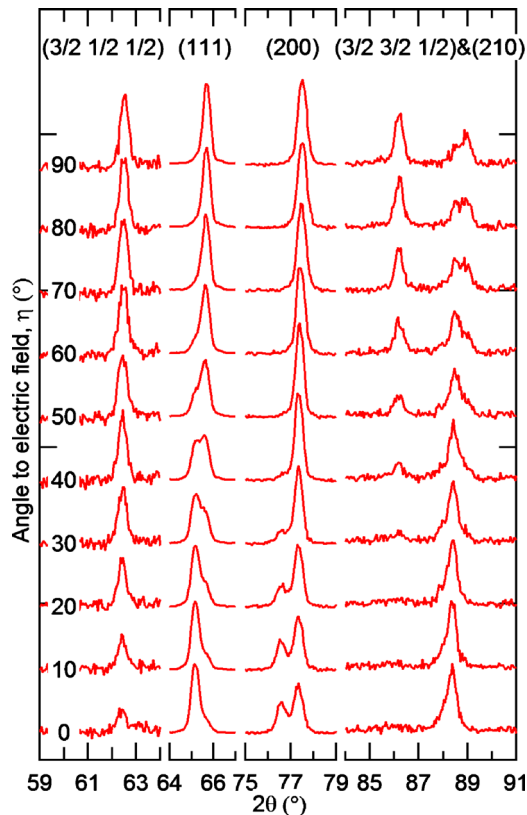
FIG. 4. (Color online) Structural variation as a function of angle (η) to the applied electric field for the poled sample, collected at 2.44 Å.

Pronounced splitting of the (200)/(002) peaks was observed as η approached 0°, indicating a tetragonal distortion. The long c-axis was preferentially oriented parallel with the electric field vector as observed in poled tetragonal $Pb(Zr_{0.52}Ti_{0.48})TiO_3$ (Refs. 6 and 25) and BNT-7BT under electric field.[10] Further peak splitting occurred in the $(111)/(1\bar{1}1)$ peaks with the long axis induced parallel to the electric field vector. This rhombohedral lattice distortion was not observed in previous x-ray data, most likely due to the sensitivity of the structure to small compositional changes near the MPB. The concurrent tetragonal and rhombohedral distortions observed here are consistent with the results of Kling *et al.*,[9] and contribute to the large electric-field-induced strain and polarization given in Table I.

This study has demonstrated that the application of an electric field to 94BNT-6BT causes significant structural transformations to occur, a result consistent with the large remanent strains observed in this system.[14] In this process, the virgin structure, which contained fractions of the $a^0a^0c^+$ and $a^-a^-a^-$ tilt systems, transformed to a strongly $a^-a^-a^-$-tilted structure, which preferentially nucleated perpendicular to the electric field. Furthermore, the poled material contained both rhombohedral and tetragonal lattice distortions, where the long axes of both structures nucleated parallel to the electric field. These electric-field-induced structural effects combine to significantly contribute to the macroscopic remanent polarization and strain of this composition. It is expected that the current results will lead to an improvement in the current understanding of high-strain phenomena in similar systems.

[1] T. Takenaka and H. Nagata, J. Eur. Ceram. Soc. **25**, 2693 (2005).
[2] J. Rödel, W. Jo, K. T. P. Seifert, E. M. Anton, and T. Granzow, J. Am. Ceram. Soc. **92**, 1153 (2009).
[3] T. Takenaka, K.-i. Maruyama, and K. Sakata, Jpn. J. Appl. Phys., Part 1 **30**, 2236 (1991).
[4] C. Xu, D. Lin, and K. W. Kwok, Solid State Sci. **10**, 934 (2008).
[5] M. Chen, Q. Xu, B. H. Kim, B. K. Ahn, J. H. Ko, W. J. Kang, and O. J. Nam, J. Eur. Ceram. Soc. **28**, 843 (2008).
[6] B. Jaffe, W. R. Cook, and H. Jaffe, *Piezoelectric Ceramics* (Academic, London, 1971).
[7] J. E. Daniels, W. Jo, J. Rödel, and J. L. Jones, Appl. Phys. Lett. **95**, 032904 (2009).
[8] W. Ge, H. Cao, J. Li, D. Viehland, Q. Zhang, and H. Luo, Appl. Phys. Lett. **95**, 162903 (2009).
[9] J. Kling, X. Tan, W. Jo, H.-J. Kleebe, H. Fuess, and J. Rödel, J. Am. Ceram. Soc. **93**, 2452 (2010).
[10] M. Hinterstein, M. Knapp, M. Hölzel, W. Jo, A. Cervellino, H. Ehrenberg, and H. Fuess, J. Appl. Crystallogr. **43**, 1314 (2010).
[11] G. Picht, J. Töpfer, and E. Hennig, J. Eur. Ceram. Soc. **30**, 3445 (2010).
[12] A. J. Royles, A. J. Bell, A. P. Jephcoat, A. K. Kleppe, S. J. Milne, and T. P. Comyn, Appl. Phys. Lett. **97**, 132909 (2010).
[13] S. Gorfman and P. A. Thomas, J. Appl. Crystallogr. **43**, 1409 (2010).
[14] J. E. Daniels, W. Jo, J. Rödel, V. Honkimäki, and J. L. Jones, Acta Mater. **58**, 2103 (2010).
[15] S.-T. Zhang, A. B. Kounga, E. Aulbach, W. Jo, T. Granzow, H. Ehrenberg, and J. Rödel, J. Appl. Phys. **103**, 034108 (2008).
[16] A. M. Glazer, Acta Crystallogr., Sect. B: Struct. Crystallogr. Cryst. Chem. **28**, 3384 (1972).
[17] G. O. Jones and P. A. Thomas, Acta Crystallogr., Sect. B: Struct. Sci. **58**, 168 (2002).
[18] V. Dorcet, G. Trolliard, and P. Boullay, Chem. Mater. **20**, 5061 (2008).
[19] G. Trolliard and V. Dorcet, Chem. Mater. **20**, 5074 (2008).
[20] J. Suchanicz, J. Kusz, H. Böhm, H. Duda, J. P. Mecurio, and K. Konieczny, J. Eur. Ceram. Soc. **23**, 1559 (2003).
[21] C. W. Tai and Y. Lereah, Appl. Phys. Lett. **95**, 062901 (2009).
[22] A. M. Balagurov, E. Y. Koroleva, A. A. Naberezhnov, V. P. Sakhnenko, B. N. Savenko, N. V. Ter-Oganessian, and S. B. Vakhrushev, Phase Transitions **79**, 163 (2006).
[23] K.-D. Liss, B. Hunter, M. Hagen, T. Noakes, and S. Kennedy, Physica B **385–386**, 1010 (2006).
[24] L. A. Schmitt, M. Hinterstein, H.-J. Kleebe, and H. Fuess, J. Appl. Crystallogr. **43**, 805 (2010).
[25] A. Pramanick and J. L. Jones, IEEE Trans. Ultrason. Ferroelectr. Freq. Control **56**, 1546 (2009).